OncoTargets and Therapy

Dovepress
open access to scientific and medical research

Open Access Full Text Article

ORIGINAL RESEARCH

Unraveling the Mechanism of Curculiginis Rhizoma in Suppressing Cisplatin Resistance in Non-Small Cell Lung Cancer: An Experimental Study

Xin Huang[1,*], Meng Wang[1,*], Baochen Zhu[1,*], Yu Hao[2], Ruoyu Gao[2], Wenhui Liu[2], Jiaojiao Cheng[1], Guodong Hua[1], Chunmiao Xue[1]

[1]Dongzhimen Hospital, Beijing University of Chinese Medicine, Beijing, People's Republic of China; [2]School of Chinese Materia Medica, Beijing University of Chinese Medicine, Beijing, People's Republic of China

*These authors contributed equally to this work

Correspondence: Guodong Hua; Chunmiao Xue, Email zhaojhuagd@126.com; xuechunmiao9501@163.com

Introduction: Non-small cell lung cancer (NSCLC) stands as one of the most prevalent malignancies, and chemotherapy remains the primary treatment for advanced stages. However, the high expression of ABC binding cassette transporters, including MRP, P-gp, and LRP, along with multidrug resistance proteins, has been identified as a significant factor contributing to decreased chemotherapy drug sensitivity. This study aims to explore the impact and underlying mechanisms of Curculiginis Rhizoma [Hypoxidaceae; Curculigo orchioides Gaertn.] (CR) in combination with cisplatin on improving chemoresistance mediated by ABC binding cassette transporters and multidrug resistance proteins in NSCLC.

Methods and Results: To unravel the relationship between JNK, MRP, P-gp, and LRP in NSCLC and gain insights into the regulatory mechanism of CR, this study employs an integrated approach encompassing bioinformatics, molecular docking, molecular dynamics, animal and cellular experiments. Bioinformatics analysis revealed a significant increase in the expression levels of JNK, MRP, P-gp, and LRP subtypes in multidrug-resistant non-small cell lung cancer. Subsequent animal experiments have shown that the combination of CR with cisplatin can improve the survival rate of lung cancer mice. Molecular docking and molecular dynamics analyses demonstrated favorable binding interactions between curculigoside and the aforementioned subtypes of JNK, MRP, P-gp, and LRP. In cellular experiments, the combination of cisplatin with both curculigoside and CR extract resulted in a notable decrease in cell viability and downregulation of the expression of JNK1, JNK2, MRP1, MRP2, MRP4, P-gp, and LRP1 in A549/cis cells.

Conclusion: Remarkably, curculigoside exerted a significant downregulation effect on the expression levels of JNK1, MRP1, MRP2, MRP4, and LRP1. CR, particularly its main effective metabolite, curculigoside, has the potential to enhance the sensitivity of non-small cell lung cancer to cisplatin by regulating levels of JNK/MRP/LRP/P-gp and mitigating multidrug resistance.

Keywords: non-small cell lung cancer, curculiginis rhizoma, CR, curculigoside, multidrug resistance, cisplatin resistance, ABC binding cassette transporter, multidrug resistance proteins

Introduction

Non-small cell lung cancer (NSCLC) is a common and aggressive subtype of lung cancer, characterized by high malignancy, recurrence risk, and heightened sensitivity to radiotherapy and chemotherapy. Despite the advancements in treatment modalities, such as chemotherapy, molecular targeted therapies, and immune checkpoint inhibitors, drug resistance remains a significant obstacle in the management of NSCLC. Multidrug resistance proteins, including multidrug resistance protein (MRP), P-glycoprotein (P-gp), and lung resistance-associated protein (LRP), are pivotal downstream regulators involved in the development of secondary multidrug resistance in NSCLC.[1–3] These transporters hinder drug entry into cancer cells, leading to diminished drug sensitivity and reduced treatment efficacy.

Received: 15 November 2023
Accepted: 28 May 2024
Published: 12 June 2024

ABC transporters are proteins that can use the energy generated by ATP hydrolysis for transmembrane transport of different substrates. These proteins are typically located on the cell membrane and can protect cells from harmful toxins.[4] Moreover, ABC transporters are energy-dependent transport systems for periplasmic solute-binding proteins (SBPs), activated by ATP hydrolysis,[5] which can transport solutes from the inside of the cell to the outside. Up to now, based on the sequences and structures of ABC domains, 48 members of the ABC transporter protein family have been identified and classified into seven families, labeled A to G. ABC transporters are further categorized into three types: importers (in prokaryotes), exporters (in eukaryotes and prokaryotes), and ABCs involved in DNA repair and translation. Therefore, they can also affect the pharmacokinetics of chemotherapy.[6] Among them, multidrug resistance protein 1 (MDR1), also known as p-glycoprotein(P-gp), has a gene named ABCB1. The gene for multidrug resistance-associated protein (MRP) is ABCC.[7] LRP is different from MRP and P-gp. It is mainly distributed in the nucleus or cytoplasm, but in lung cancer cells, it is mainly distributed in cytoplasmic vesicles. It mainly prevents drugs from entering the nucleus through nuclear pores, transports drugs that have entered the nucleus out of the cell or transfers drugs in the cytoplasm to vesicles, and excretes them through exocytosis, resulting in drug resistance reactions in the body.[8] Studies have found that targeting the inhibition of the expression of P-gp, MRP and LRP proteins in tumor tissues can enhance the sensitivity of non-small cell lung cancer to chemotherapy drugs and improve the tumor inhibition rate.[9,10]

To address the challenge of multidrug resistance in NSCLC, comprehensive exploration of the underlying mechanisms and identification of predictive biomarkers at the molecular level are essential. In clinical practice, combination therapy has been adopted to optimize NSCLC treatment outcomes. In particular, the integration of traditional Chinese medicine (TCM) with Western medicine has shown significant advantages in enhancing treatment success rates, improving survival outcomes, and alleviating patient suffering. As a result, the combined approach is gaining increasing attention as a promising strategy for combating NSCLC drug resistance.

Curculiginis Rhizoma [Hypoxidaceae; Curculigo orchioides Gaertn.] (CR) is a prominent medicinal botanical drug deeply rooted in Traditional Chinese Medicine (TCM). With its rich history of use, CR has gained recognition for its diverse pharmacological properties and therapeutic applications. CR exhibits promising pharmacological effects as an anti-tumor and immune-modulatory agent.[11,12] Our previous research revealed that CR extract and its main metabolite sensitize cisplatin-resistant lung cancer cells (A549/cis) to cisplatin treatment and downregulate P-glycoprotein (P-gp) expression in A549/cis.[13] Building on these findings, this study aims to further investigate the roles of CR and Curculigoside in overcoming cisplatin resistance in non-small cell lung cancer (NSCLC) using an integrated approach that includes bioinformatics analysis, network pharmacology, molecular docking, molecular dynamics simulations, and in vivo and in vitro experiments. The ultimate goal is to identify novel traditional Chinese medicine monomers for the reversal of multidrug resistance in NSCLC, supporting the potential of combining traditional Chinese medicine with Western medicine in cancer therapy.

Materials and Methods

Ethnopharmacological Relevance

Curculiginis Rhizoma [Hypoxidaceae; Curculigo orchioides Gaertn.], is a traditional Chinese medicine with efficacy of tonifying Yang and strengthening body immunity in thousands of years of clinical practice in China. Curculigoside is a major active metabolite of Curculiginis Rhizoma, which plays an important role in anti-inflammatory, anti-oxidation and immune-enhancing.

Animal Model Establishment

Establishment of in situ lung cancer model mice: Male C57BL/6 mice (18–22 g, supplied by Beijing Vital River Laboratory Animal Technology Co., Ltd) were acclimatized for 3 days before the experiment. Mixed the mouse Louis lung cancer cells (LLC cells, the cell concentration is $1\times10^{6}\cdot mL^{-1}$) with Matrigel matrix glue and loaded into 80 liters/unit insulin syringe. Anesthetized and fixed the mice. After disinfection, pre-prepared cell suspension was injected into left axillary region of mice. Normally fed for 2 weeks.

Animal Treatment

Mice were housed in the specific-pathogen-free facility at the laboratory of Dongzhimen Hospital, Beijing University of Chinese Medicine. All the experiments on animals were performed under the Guidelines for the Care and Use of Laboratory Animals. The protocols were approved by the institutional animal experimentation committee of Dongzhimen Hospital, Beijing University of Chinese Medicine.

Mice were divided into 5 groups: Normal group, cisplatin group, and the combination treatment groups with high, medium, and low concentrations of CR along with cisplatin (Jiangsu Hansoh Pharmaceutical Group Co., Ltd. Batch number: H20040813) (The concentration of cisplatin was 2.5mg/mL, and each mouse was injected intraperitoneally at 0.1mL/10g every other day; High-dose CR: CR water extract at a concentration of 8mg/mL, administered via gavage at 0.05mL/g, every other day; Medium-dose CR: CR water extract at 4mg/mL, administered via gavage at 0.05mL/g every other day; Low-dose CR: CR water extract at a concentration of 2mg/mL, administered via gavage at 0.05mL/g, every other day).

Bioinformatics Analysis

The combined expression profiles and clinical data of TCGA-LUSC and TCGA-LUAD were downloaded from TCGA[14] database for analysis. For cancer drug sensitivity information, normal samples were excluded, leaving a total of 1043 patient samples. Samples exhibiting Complete Response were considered drug-sensitive, while those showing Non-Complete Response, including partial response, stable disease, and progressive disease, were regarded as drug-resistant,[15] comprising 161 chemotherapy-resistant samples and 218 chemotherapy-sensitive samples. Among these samples, 623 were in survival status, while 399 were in death status.

GSE109821[16] and GSE77209[17] datasets, along with their corresponding drug sensitivity information, were obtained from the GEO database. GSE109821, sourced from the non-small cell lung cancer cell line on the sequencing platform GPL11154, included 36 samples, with 4 samples classified as chemotherapy-resistant and 32 samples as chemotherapy-sensitive. GSE77209, sourced from the non-small cell lung cancer cell line on the sequencing platform GPL10558, comprised 28 samples, with 18 samples classified as chemotherapy-resistant and 10 samples as chemotherapy-sensitive. The above two GEO data sets were combined into one set of data for analysis by using R package sva[18] to correct the batch effect existing between different data sets.

JNK, MRP, P-gp, and LRP genes may exhibit differential expression patterns between drug-resistant and drug-sensitive samples. To explore this, we utilized the R package ggpubr[19] to visually represent the expression profiles and corresponding drug sensitivity information obtained from TCGA and GEO databases using violin plots, with samples grouped into resistant and sensitive categories. The Mann–Whitney *U*-test was performed to determine statistical significance, with $P < 0.05$ considered as statistically significant. Moreover, TCGA expression profiles and clinical data were employed to segregate cancer patient samples into high- and low-expression groups based on the expression and survival information of JNK, MRP, P-gp, and LRP-related genes using the R package survminer[20] and its surv_cutpoint function.[21] Subsequently, we performed Kaplan–Meier (KM) survival analysis using the R packages survival[22] and survminer[20] to compare overall survival (OS) between the high- and low-expression groups. The results were visualized by plotting survival curves, and statistical significance was assessed using the Log rank test.

Molecular Docking Analysis

The 3D structure of the curculigoside was retrieved from the PubChem database and downloaded in SDF format. Subsequently, the SDF format file was converted to a PDB format file using PyMol. Following this, the ligand small molecules were imported into AutoDock Tools software and subjected to dehydration, hydrogenation, and detection of rotatable bonds before being saved in PDBQT format to construct the active component molecular library. Concurrently, the protein 3D crystal structure PDB files of JNK1, JNK2, MRP1, MRP2, MRP4, P-gp, and LRP1 were obtained from the PDB protein database. These protein structures underwent processing in AutoDockTools, involving the addition of polar hydrogen, fixing atom type, fixing bond order, adding charge, setting protonation state, and removing additional water molecules, followed by saving the processed structures in "pdbqt" format files.

First, LibDock molecular docking was performed with the Conformation Method set to Fast and Docking Preferences set to High Quality. The initial evaluation of ligand-receptor binding was based on the docking results. Subsequently, AutoDock Vina software was used to perform molecular docking of curculigoside with JNK1, JNK2, MRP1, MRP2, MRP4, P-gp, and LRP. The docking box size was set to 88 Å × 88 Å × 82 Å to cover all docking sites. The docking process was conducted using a semi-flexible docking approach, where JNK1, JNK2, MRP1, MRP2, MRP4, P-gp, and LRP were treated as rigid bodies, while only the conformation of the ligand small molecule was allowed to vary.

Molecular Dynamics Analysis

The protein and small-molecule ligand of molecular docking results were separated. The small-molecule force field files were subsequently generated using the antechamber tool in Ambertools software. These small-molecule force field files were then converted into GROMACS force field files using the acpype software tool. Finally, the protein and small-molecule ligand files were merged to construct the simulation system for the complex.

Molecular dynamics simulations (MD) were performed using Gromacs 2022 program under constant temperature and pressure with periodic boundary conditions. The Amber99sb-ildn force field and TIP3P water model were employed. During the MD simulations, all hydrogen bonds were constrained using the LINCS algorithm with a time step of 2 fs. Electrostatic interactions were computed using the Particle-mesh Ewald (PME) method with a cutoff of 1.2 nm. The cutoff for van der Waals interactions was set to 10 Å, and the neighbor list was updated every 10 steps. The V-rescale temperature coupling method was used to maintain the simulation temperature at 295 K, and the Berendsen method was used to control the pressure at 1 bar. NVT and NPT equilibration simulations were performed for 100 ps at 295 K, followed by a 100 ns MD simulation of the complex system with conformations saved every 10 ps. After the simulation, the trajectories were analyzed using VMD and PyMOL, and the g_mmpbsa program was used for MMPBSA binding free energy analysis between the protein and small-molecule ligands.

Botanical Drug Preparation Methods

The original medicinal materials of CR were provided by Beijing Shengshilong Pharmaceutical Co. LTD (Batch number: 201018gxw). The extract of CR was prepared through the following steps: Weighed 64.6g of CR, placed it in a round-bottom flask, added 646mL of distilled water, and refluxed for 90 minutes. After double-layer gauze filtration, the residue was subjected to a second reflux with 516.8mL of distilled water for 60 minutes. The extracts from both steps were combined, and the solution was evaporated at 60°C to obtain 16.88g of dried extract (extract ratio 1:3.827). To use, dissolve the extract in distilled water to prepare a stock solution with a concentration of 0.128g/mL.

Curculigoside was provided from Shanghai Yuanye Bio-Technology Co. Batch number: A10194-20mg, Analytical standard, Content 98.3%. When using it, dissolve curculigoside in cell culture medium to prepare a stock solution with a concentration of 1mg/mL.

Cell Culture

The human cisplatin-resistant lung cancer cell line A549/cis cells were obtained from the Cell Resource Center, Institute of Basic Medical Sciences, Chinese Academy of Medical Sciences (Resource number:1101HUM-PUMC000519). The cells were cultured in RPMI1640 medium (Beijing Solarbio Science&Technology Co., Ltd., China) supplemented with 15% fetal calf serum (Biological Industries, IL) and 100 units/mL penicillin and streptomycin (Invitrogen, Waltham, MA, USA). Cell cultures were maintained in a 37°C, 5% CO_2 incubator with saturated humidity. The cells were passaged every 4 days at a ratio of 1:4 and used for experiments during the logarithmic growth phase.

Cell Viability

A549/cis cells were seeded in 96-well plates and incubated in a 37°C, 5% CO_2 incubator. The growth of A549/cis cells was observed under an inverted microscope. Adherent culture cells were washed with PBS, and 5×10^3 cells (100μL suspension) were then seeded in each well of the 96-well plates. In single-agent administration experiments, the cells were treated with cisplatin alone at a concentration of 1μg/mL, 2μg/mL, 3μg/mL, 4μg/mL, 5μg/mL, 6μg/mL, 7μg/mL, 10μg/mL, CR at a concentration of 100μg/mL, 250μg/mL, 500μg/mL, 750μg/mL, 1000μg/mL, and curculigoside at

a concentration of 0.5μg/mL, 1μg/mL, 5μg/mL, 10μg/mL, 20μg/mL, 50μg/mL, 100μg/mL, 500μg/mL, incubated for 24 hours. In combination administration experiments, the cells were treated with cisplatin at a concentration of 6μg/mL, CR at concentrations of 50μg/mL, 500μg/mL, and 1000μg/mL, and curculigoside at concentrations of 50μg/mL, 500μg/mL, and 1000μg/mL in complete medium, and then incubated for 24 hours. After the incubation, the medium was aspirated, and each well was added with 10μL of CCK-8 reagent (Dongren Chemical Technology, Shanghai, China; Batch number: CK04) and 90μL of complete medium solution. The plates were further incubated at 37°C for 1 hour. After incubation, the absorbance of each well was measured at a wavelength of 450nm using a microplate reader. The experiment was repeated three times. The inhibition rate (%) was calculated using the following formula: Inhibition rate (%) = [(A_blank group - A_observation group)/(A_blank group - A_solvent control group)] × 100%.

Western Blotting Analysis

Following a 24-hour treatment of A549/cis cells with the aqueous extract of CR (500μg/mL) and curculigoside (50μg/mL), both individually and in combination with cisplatin (6μg/mL), the treated A549/cis cells were subsequently incubated in RIPA buffer (RIPA:PMSF=10:1) for a duration of 30 minutes. Followed by centrifugation at 12,000 x g for 15 minutes at a temperature of 4°C. Total protein was extracted from cultured cells using RIPA buffer, supplemented with the PMSF protease inhibitor (Beijing Solarbio Science&Technology Co., Ltd.; Batch number: P8340). The protein concentration was determined using the BCA Protein Assay kit (Beijing Solarbio Science&Technology Co., Ltd.; Batch number: PC0020). Subsequently, 25μg of total protein lysates were subjected to electrophoresis on a 7.5% SDS-polyacrylamide gel (Beijing Solarbio Science&Technology Co., Ltd.; Batch number: P1200). Following separation on SDS-PAGE gels, the proteins were transferred onto PVDF membranes (Merck Millipore Ltd; batch number: R1CB66016). Subsequently, the membranes were blocked with 5% skim milk at room temperature for a duration of 1 hour. Afterward, they were washed three times with TBST and incubated overnight at 4°C with a diluted primary antibody JNK1 (1:5000, Abcam, product number: ab110724), JNK2 (1:500, Abcam, product number: ab76125), MRP1 (1:1000, Abcam, product number: ab230948), MRP2 (1:500, Abcam, product number: ab172630), MRP4 (1:1000, Abcam, product number: ab233382), P-gp (1:500, Abcam, product number: ab170904), LRP1 (1:1000, Abcam, product number: ab92544), and GA (1:5000, Abways, product number: AB0037). Following this, the membranes were washed three times for five minutes each with TBST and then incubated with a secondary Goat Anti-Rabbit IgG(H + L)HRP (1:10,000, Abways, product number: AB0101) at room temperature for 1 hour. Finally, the membranes were washed three times with TBST at room temperature for 5 minutes each time. The target protein was detected by ECL reagent (Beijing Ranjeco Technology Co., LTD., batch number: 21,299,536), and the intensity of protein bands was quantified by Image J software.

Measurement of Rhodamine 123 Concentration

Following a 24-hour treatment of A549/cis cells with the aqueous extract of CR (500μg/mL) and curculigoside (50μg/mL), both individually and in combination with cisplatin (6μg/mL) in 6-well plates. After digestion with trypsin without EDTA (Thermo Fisher Scientific Inc.; Batch number: 15,050,065), the cells were stained with Rhodamine 123 dye (GluBio Pharmaceutical Co., Ltd; Batch number: R-22420) at room temperature in the dark for 30 minutes. Following a centrifugation at 1000g for 5 minutes, the supernatant was removed. The cells were then washed twice with PBS, each for 5 minutes, and resuspended in PBS for confocal microscopy observation at 40x magnification with an emission wavelength of 529nm.

Statistical Analysis

Statistical analysis was performed using SPSS 20.0. A two-way ANOVA followed by Bonferroni's multiple comparisons test was used to compare differences between multiple groups. Two-tailed unpaired Student's t tests were performed and p-values <0.05 were considered significant. All statistical tests are justified as appropriate, and the data meet the assumptions of the tests.

Results

The Anti-Cancer Effects of CR in vivo

Twelve days after the in situ injection of LLC cells into the mice, tumor tissue was visible in the armpit area. The results indicate that compared to the cisplatin group, the survival time of C57 mice was significantly prolonged after administering cisplatin in combination with high and medium concentrations of CR, as shown in Figure 1.

The Expressions of JNK1, JNK2, MRP1, MRP4, P-Gp and LRP1 in NSCLC Were Analyzed by Bioinformatics

Using the GEO database, violin plots were generated based on the expression values of JNK, MRP, P-gp, and LRP-related genes in drug-resistant and drug-sensitive samples. The results indicated significant differences in the expression levels of JNK1, JNK2, MRP1, MRP4, P-gp, and LRP1, while no significant differences were observed for MRP2 (Figure 2).

Subsequently, the TCGA database was utilized to analyze JNK, MRP, P-gp, and LRP-related genes. The results showed significant differences in the expression levels of JNK2, MRP1, MRP4, and LRP1, while no significant differences were observed for JNK1, MRP2, and P-gp (Figure 3).

Based on the optimal threshold of JNK, MRP, P-gp, and LRP-related gene expression in relation to survival status, patients were divided into high-expression and low-expression groups. Survival analysis revealed that the overall survival rate was worse in the high JNK1, JNK2, MRP2, and LRP1 expression groups. Additionally, the overall survival rate was worse in the low MRP4 and P-gp expression groups. However, there was no significant difference in overall survival between the high MRP1 expression and low MRP1 expression groups. These findings suggest that JNK1, JNK2, MRP2, MRP4, and LRP1 may impact the prognosis of non-small cell lung cancer (NSCLC) patients (Figure 4).

Molecular Docking and Molecular Dynamics Showed That Curculigoside Had Good Binding Ability with JNK1, JNK2, MRP1, MRP4, P-Gp and LRP1

Molecular docking analysis demonstrated favorable binding interactions between curculigoside and JNK1, JNK2, MRP1, MRP4, P-gp, and LRP1. The corresponding docking scores for curculigoside with JNK1, JNK2, MRP1, MRP2, MRP4, MDR1(P-gp), and LRP were −6.79 kcal/mol, −7.51 kcal/mol, −6.49 kcal/mol, −6.89 kcal/mol, −7.62 kcal/mol, −8.12 kcal/mol, and −6.05 kcal/mol, respectively, indicating strong interactions and good docking activity (Figure 5).

Considering that molecular docking may not fully account for protein flexibility, molecular dynamics simulations were conducted to further elucidate the interaction between curculigoside and receptor proteins. As depicted in (Figure 6A–C), the Root mean square deviation (RMSD) values of curculigoside and its binding partners (JNK1, JNK2, MRP1, MRP2, MRP4, P-gp, and LRP) remained relatively stable during the 100ns molecular dynamics simulations. Additionally, the Radius of Gyration (Rg) values indicated overall stability, suggesting that the protein-small

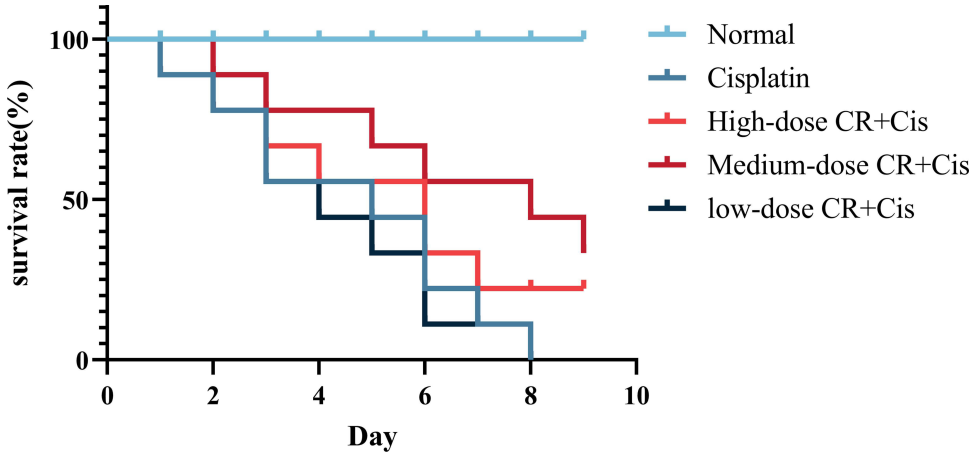

Figure 1 Survival curve of C57 mice.

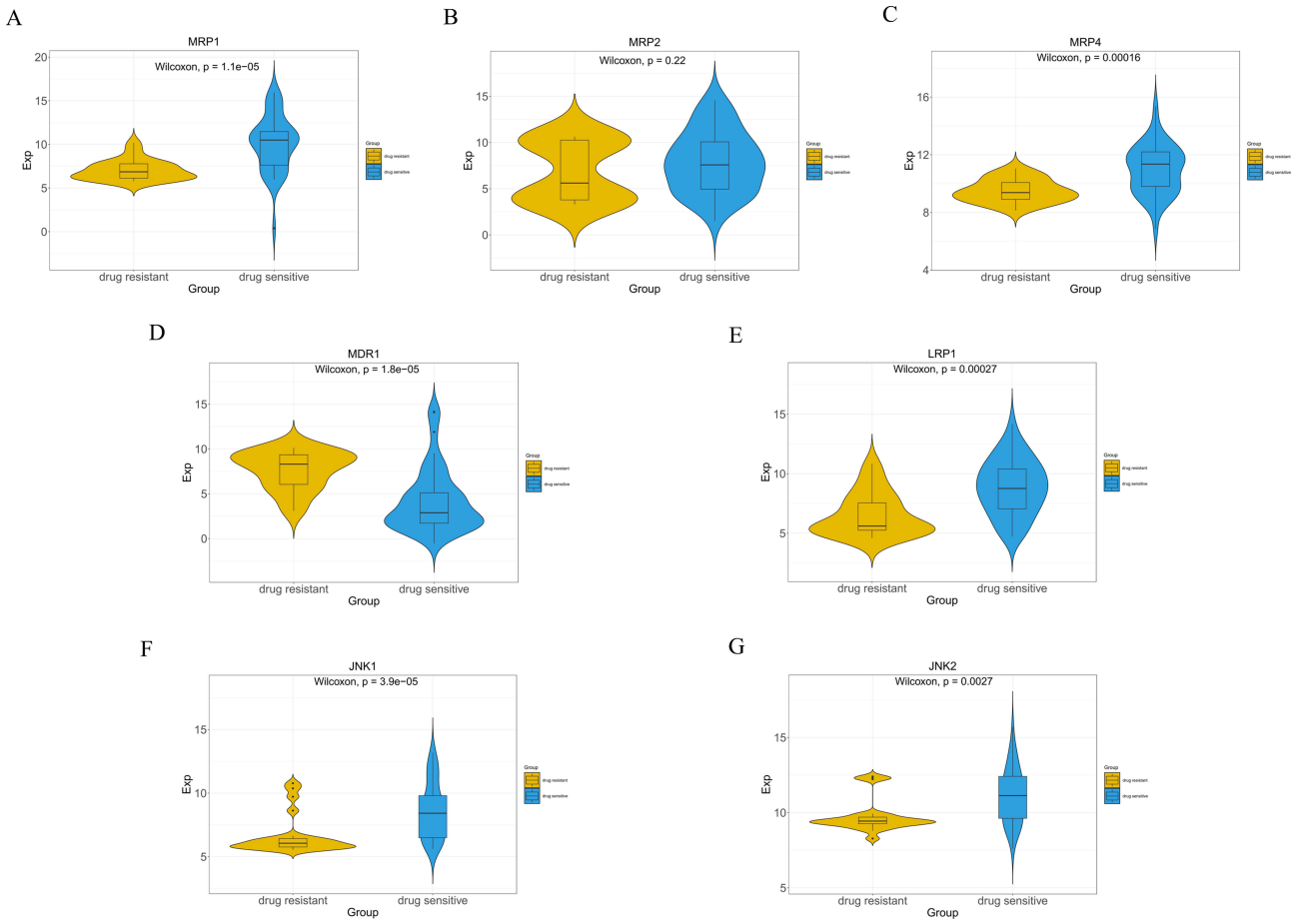

Figure 2 The expressions of JNK1, JNK2, MRP1, MRP2, MRP4, P-gp and LRP1 in NSCLC were analyzed by GEO Database. Violin plots illustrating the expression differences of each protein between the drug-sensitive group and drug-resistant group. (**A**) MRP1, (**B**) MRP2, (**C**) MRP4, (**D**) P-gp (MDR1), (**E**) LRP1, (**F**) JNK1, (**G**) JNK2.

molecule complexes remained stable during the simulations. Analysis of the distance between the centroid of the initial docking site residues and the centroid of curculigoside provided information on the stability of the small-molecule binding to the protein during the simulations (Figure 6D). Moreover, the analysis of the embedding area indicated that the binding state of curculigoside and proteins remained relatively stable (Figure 6E), except for fluctuating hydrogen bonds between curculigoside and LRP (Figure 6F). The number of hydrogen bonds in the other groups was relatively stable, primarily distributed between 2 and 6 (Figure 6G).

Considering solvation energy, RMSD, Rg, and interaction energy for each group, the trajectory of the complex in the steady state was selected and calculated using the Molecular Mechanics-Poisson Boltzmann Surface Area (MM-PBSA) method (Table 1). The binding energy of curculigoside to JNK1, JNK2, MRP1, and MRP4 was negative, indicating strong binding and affinity between curculigoside and these proteins. Conversely, the binding energy of curculigoside to LRP, MDR1(P-gp), and MRP2 was positive, suggesting weaker binding and affinity in these cases. The binding free energy decomposition revealed that van der Waals force interaction was the primary driving force for curculigoside binding to the receptor proteins, followed by electrostatic interaction, with hydrophobic interactions playing an auxiliary role.

On this basis, the affinity between curculigoside and the protein was analyzed. By superposing the small molecule to the simulated conformation of the protein, it was found that the small molecules in each complex had a high degree of overlapping conformation near the initial binding site. The results showed that the small molecules were always bound to and near the initial binding site of the protein during the simulation. Finally, the conformation when the simulation is stable is selected to analyze its structure and interactions, as shown in Figure 7.

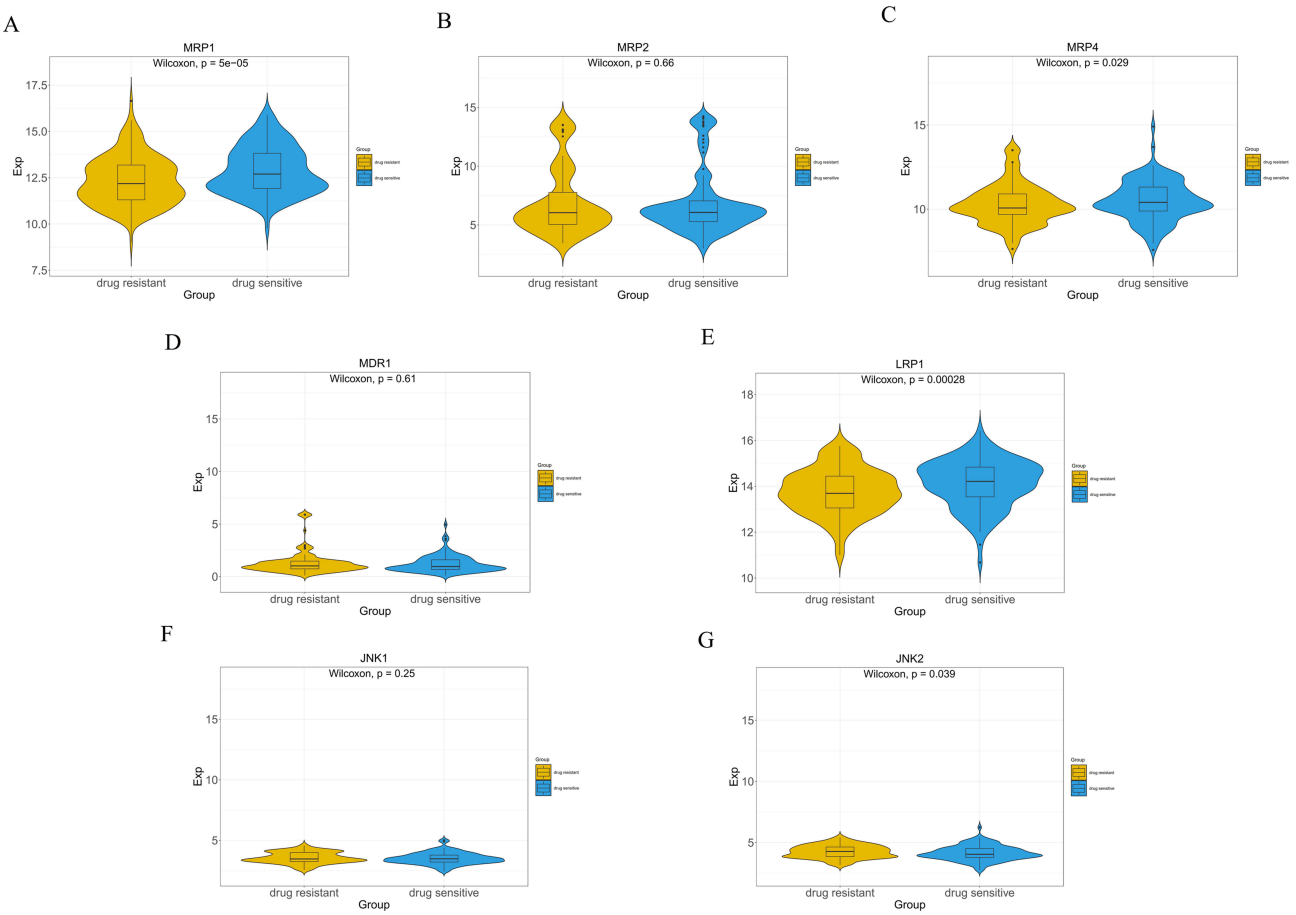

Figure 3 The expressions of JNK1, JNK2, MRP1, MRP2, MRP4, P-gp and LRP1 in NSCLC were analyzed by TCGA Database. Violin plots illustrating the expression differences of each protein between the drug-sensitive group and drug-resistant group. (**A**) MRP1, (**B**) MRP2, (**C**) MRP4, (**D**) P-gp (MDR1), (**E**) LRP1, (**F**) JNK1, (**G**) JNK2.

Cisplatin Combined with CR/Curculigoside Inhibited A549/Cis Cell Proliferation

Cell viability was assessed using the CCK8 assay. Cisplatin, Curculiginis Rhizoma and curculigoside alone, it was found that Curculiginis Rhizoma and curculigoside had almost no toxic effect on A549/cis cells. Due to the toxicity of Curculiginis Rhizoma itself, the optimal concentration was selected for the following experiments after reference as shown in the Figure 8A–C. Cisplatin combined with different concentrations of Curculiginis Rhizoma water extract (50μg/mL, 500μg/mL, 1000μg/mL) and different concentrations of curculigoside (50μg/mL, 500μg/mL, 1000μg/mL) had a higher inhibition rate on A549/cis cells than cisplatin alone group. The combination group exhibits an increased inhibitory effect on A549/cis cell with the rising concentrations of CR and curculigoside. At the same time, the groups treated with CR and curculigoside alone did not show any inhibitory effects on cells, indicating that their synergistic enhancement with cisplatin may not originate from their direct cytotoxicity to the cells, as illustrated in Figure 8D and E. The reversal activities assay of CR and curculigoside on cisplatin-insensitivity of A549/DDP cells are 250 and 166.7, respectively.

Inhibition of Cisplatin-Induced Upregulation of JNK, MRP, LRP, and P-Gp by CR/Curculigoside

Western blot analysis was employed to assess protein expression levels. The findings demonstrated an upregulation of JNK1, JNK2, MRP1, MRP2, MRP4, LRP1, and P-gp protein expressions in the cisplatin group compared to the normal group. In particular, the cisplatin group exhibited significantly increased expressions of JNK1, JNK2, MRP2, MRP4, and LRP1. In contrast, the cisplatin +CR group displayed decreased expressions of JNK1, JNK2, MRP1, MRP2, MRP4, LRP1, and P-gp, with notable reductions in MRP1, MRP2, and LRP1 compared to the cisplatin group. Additionally, the

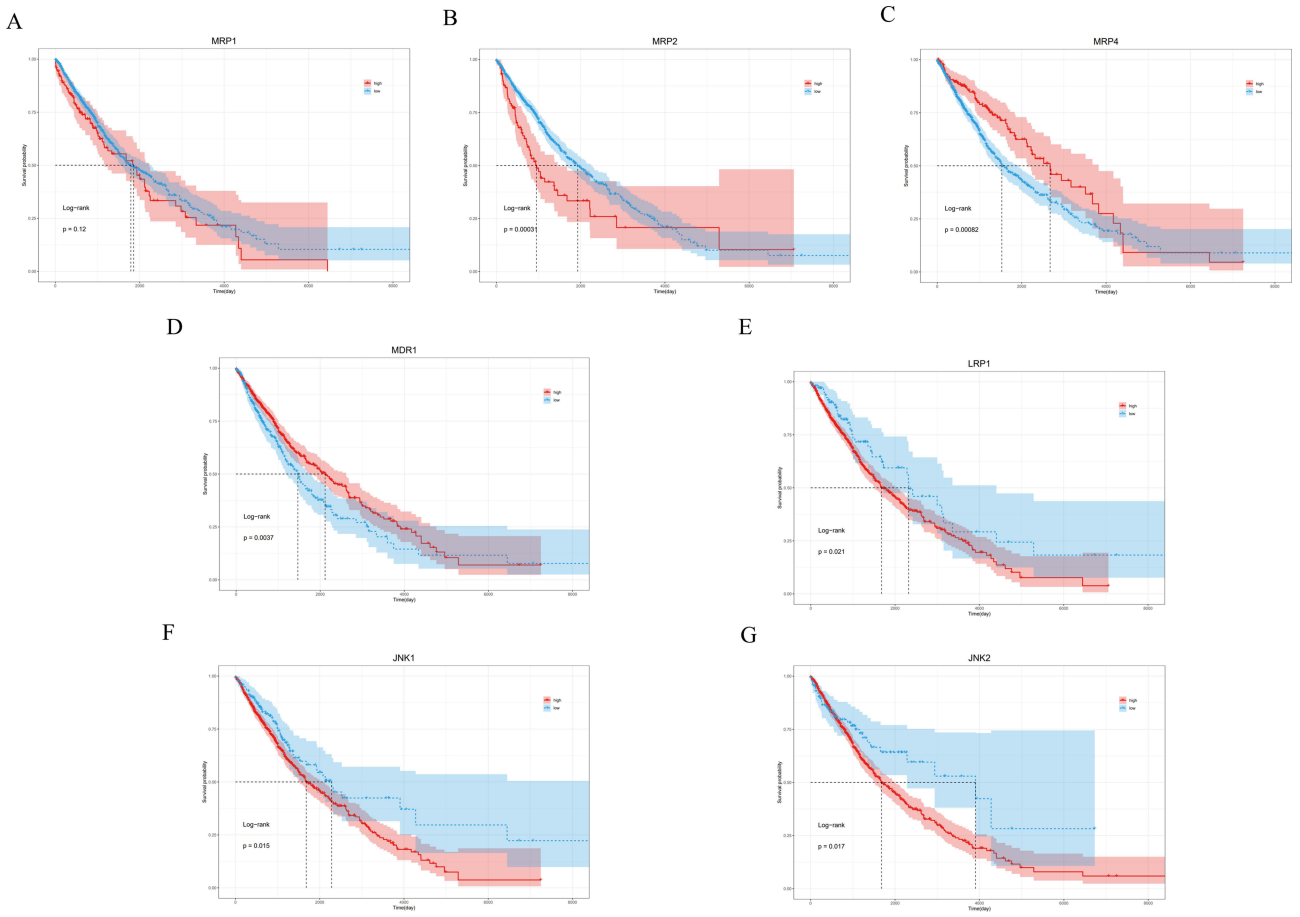

Figure 4 Survival analysis of JNK1, JNK2, MRP1, MRP2, MRP4, P-gp and LRP1 in NSCLC in TCGA database. Survival curves comparing the high expression group and low expression group of each protein. (**A**) MRP1, (**B**) MRP2, (**C**) MRP4, (**D**) P-gp (MDR1), (**E**) LRP1, (**F**) JNK1, (**G**) JNK2.

cisplatin +curculigoside group exhibited decreased expressions of JNK1, JNK2, MRP1, MRP2, MRP4, LRP1, and P-gp compared to the cisplatin group, with significant decreases observed in JNK1, MRP1, MRP2, MRP4, and LRP1. Meanwhile, compared to the normal group, there were no significant differences in the expression of JNK1, JNK2, MRP1, MRP2, MRP4, LRP1, and P-gp in the CR and curculigoside groups (Figure 9A–G).

Rhodamine 123 is Lowly Expressed in the Cells by CR/Curculigoside

Confocal fluorescence microscopy results revealed that compared to the control group, the content of Rhodamine 123 decreased in the cisplatin group, whereas there were no significant changes in the CR group and the curculigoside group. In comparison to the cisplatin group, the content of Rhodamine 123 increased in the cisplatin +CR group and the cisplatin +curculigoside group (Figure 10A–F).

Discussion

The advent of molecular targeted drugs and immunotherapy has expanded the therapeutic landscape for non-small cell lung cancer (NSCLC). While these novel treatment options show promising clinical outcomes, chemotherapy remains a crucial component due to its broad-spectrum efficacy and longstanding clinical application.[9,23] However, the emergence of multidrug resistance presents a significant obstacle, with over 70% of NSCLC patients developing resistance to platinum-based drugs within a short period, ultimately leading to treatment failure.[24] Consequently, overcoming chemotherapy resistance remains an urgent and pivotal issue in NSCLC management.

In this study, we initially observed in animal experiments that CR could reduce the mortality rate in lung cancer mice after cisplatin administration (the animal model used is a commonly internationally employed in situ animal model.[25]),

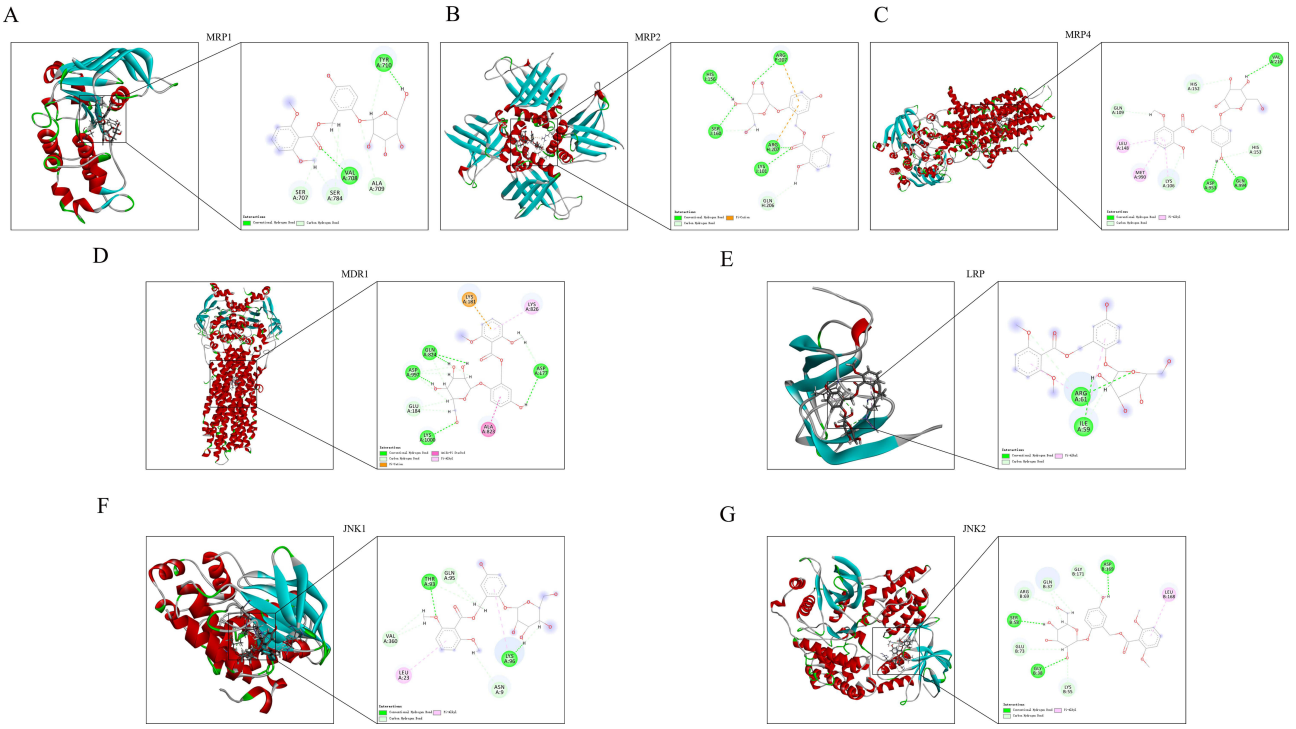

Figure 5 Molecular docking analysis of Curculigoside with JNK1, JNK2, MRP1, MRP2, MRP4, P-gp, and LRP1. Results of docking analyses of Curculigoside, in the binding pocket of each protein. The insets are 2D presentation of the binding of the metabolites. (**A**) MRP1, (**B**) MRP2, (**C**) MRP4, (**D**) P-gp (MDR1), (**E**) LRP1, (**F**) JNK1, (**G**) JNK2.

although its mechanism of action remained unclear. Combined with preliminary cell pre-experiments, we found that CR alone did not exhibit a significant inhibitory effect on tumor cells. Therefore, we hypothesized that the mechanism by which CR enhances cisplatin sensitivity may involve the suppression of cisplatin resistance. To further investigate, we employed bioinformatics analysis, molecular docking, and molecular dynamics to screen for potential targets of CR and its main metabolite, curculigoside, in combating drug resistance. Subsequently, we validated these targets through cell experiments.

Currently, the exploration of tumor multidrug resistance is shifting towards understanding the impact of genome instability, tumor heterogeneity, epigenetics, etc.[26–28] However, the primary downstream regulatory target that persists is the abnormal expression of ABC binding cassette transporters and resistance-related proteins.[29] MRP, which falls under the ABC subfamily C, operates by actively expelling negatively charged drug molecules from cells, resulting in diminished intracellular drug levels.[30,31] LRP, known for its complete positive expression in lung cancer, plays a crucial role in mediating the transportation of platinum and other antitumor drugs from the nucleus to the cytoplasm.[32] While P-gp, a member of the ABC subfamily B, also exhibits a high expression rate in NSCLC and functions by impeding the transport of nucleus-targeted drugs into the cytoplasm, followed by their subsequent sequestration into transport vesicles, culminating in exocytosis and extrusion from the cell. This orchestrated process ultimately engenders drug resistance in tumor cells.[33–36] Therefore, the resistance proteins lead to the expulsion of chemotherapy drugs from tumor cells, reduce the intracellular drug concentration, and the tumor cells up-regulate the expression of resistance proteins due to the prolongation of treatment time, which are important reasons for the failure of chemotherapy.

In our study, it was found that NSCLC drug-resistant cell lines in GEO database, MRP protein subtypes MRP1, MRP4 and LRP1, P-gp were significantly different in NSCLC drug-resistant cell lines. NSCLC-related clinical samples were obtained from TCGA database, and it was found that NSCLC patients with high JNK1, JNK2, MRP2, LRP1 expression and low MRP4, P-gp expression had poor overall survival.

Regrettably, no chemical drugs capable of clinically regulating these resistance-related proteins have been identified yet. Addressing this therapeutic gap holds promise for improving treatment outcomes in drug-resistant NSCLC cases.

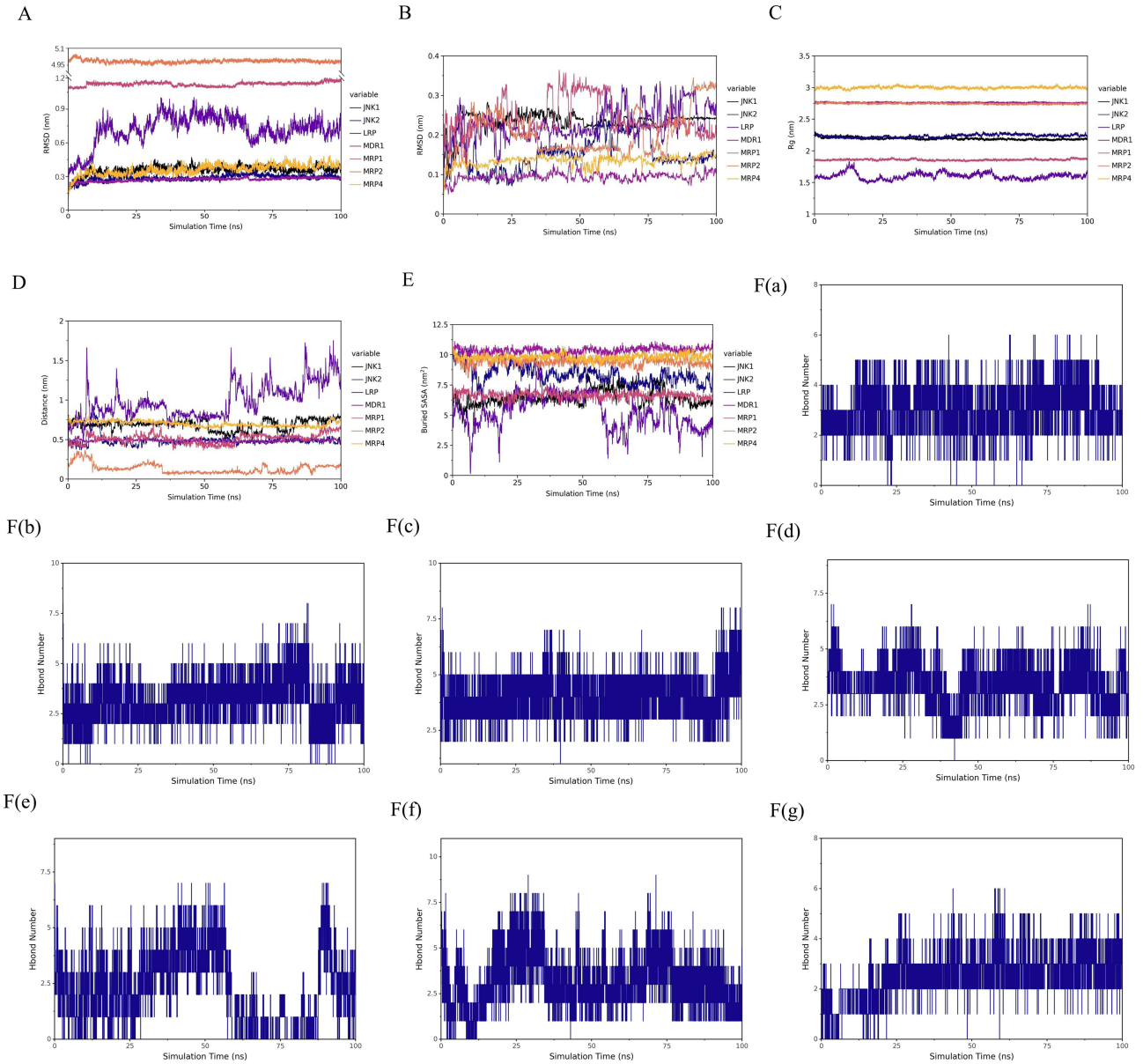

Figure 6 Molecular dynamics analysis of Curculigoside with JNK1, JNK2, MRP1, MRP2, MRP4, P-gp, and LRP1. **(A–C)**: comparison of RMSD, Rg and interaction energy stability analysis for JNK1, JNK2, MRP1, MRP2, MRP4, P-gp and LRP1; (**D**) Comparison of distance analysis between small molecule and initial binding site; (**E**) Comparison of binding state analysis of small molecules and proteins; **F(a-g)**: Analysis of hydrogen bonds between small molecules and proteins. **F(a)**: MRP1, **F(b)**: MRP2, **F(c)**: MRP4, **F(d)**: P-gp (MDR1), **F(e)**: LRP1, **F(f)**: JNK1, **F(g)**: JNK2.

Numerous clinical studies have reported that traditional Chinese medicine monomers or formulations combined with chemotherapy drugs exhibit dual benefits by reducing drug-induced adverse reactions and displaying potential chemotherapy sensitization and anti-drug resistance effects.[37–39] In light of this, our research team conducted a screening of traditional Chinese medicines, identifying CR as a promising candidate for improving chemotherapy sensitivity. Moreover, CR demonstrates favorable anti-inflammatory properties[40] and immunomodulatory effects,[41] contributing to the mitigation of chemotherapy-induced adverse reactions. Previous investigations also revealed that CR extract and its main metabolites enhance cisplatin sensitization in cisplatin-resistant lung cancer cells (A549/cis) and downregulate P-glycoprotein (P-gp) expression in A549/cis (The cisplatin-resistant cells are a classical human lung cancer cell line with significant cisplatin resistance, prepared by Cell Resource Center in China.).[13] Meanwhile, we found that administration of CR and curculigoside alone did not show inhibitory effects on A549/cis. It is speculated that their synergistic

Table 1 Energy Terms Associated with Binding Energies Between Curculigoside and JNK1, JNK2, MRP1, MRP4, P-Gp and LRP1

Complex	ΔHvdw	ΔHele	ΔHpol	ΔHnonpol	-TΔS	ΔGbind*
JNK1	−118.86	−69.926	165.721	−16.159	33.487	−5.737
JNK2	−193.774	−91.611	237.64	−20.943	29.233	−39.455
LRP	−111.14	−135.509	257.632	−18.413	35.786	28.356
MDR1	−206.621	−111.175	333.512	−28.362	21.156	8.51
MRP1	−141.923	−68.779	161.907	−17.828	30.715	−35.908
MRP2	−171.636	−126.239	319.397	−25.587	40.467	36.402
MRP4	−193.477	−118.809	260.314	−26.803	15.183	−63.592

Notes: *ΔGbind=ΔHvdw+ΔHele+ΔHpol+ΔHnonpol-TΔS.

enhancement with cisplatin may not arise from their direct cytotoxicity to the cells but rather from their potential involvement in reducing the efflux of cisplatin from the cells. Building upon these findings, we further conducted research using molecular docking and molecular dynamics techniques. The results of molecular docking revealed that curculigoside, the main effective metabolite in CR, exhibited excellent docking activities with MRP1, MRP2, MRP4, P-gp, and LRP1. Additionally, molecular dynamics simulations supported curculigoside's favorable docking with MRP1, and MRP4. Building upon this foundation, we conducted experiments utilizing curculigoside and the water extract of CR in combination with cisplatin to assess their inhibitory effects on the cisplatin-resistant lung cancer cell line A549/cis and their impact on the expression of MRP, P-gp, and LRP proteins. In comparison to cisplatin treatment alone, cisplatin

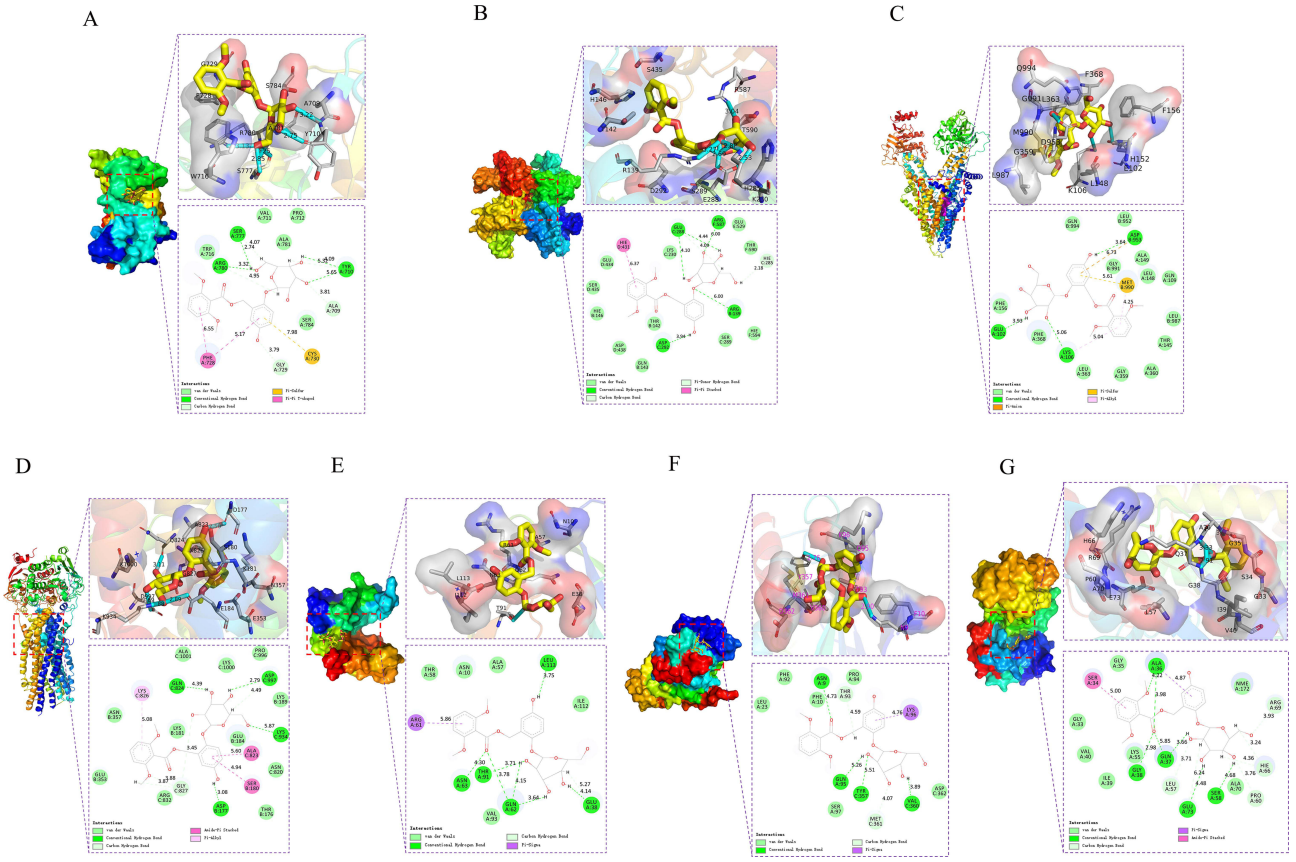

Figure 7 Affinity analysis between Curculigoside with MRP1, MRP2, MRP4, P-gp, LRP, JNK1, and JNK2. **(A–G)**: The conformation at stabilization was simulated between Curculigoside with MRP1, MRP2, MRP4, P-gp, LRP, JNK1, and JNK2.

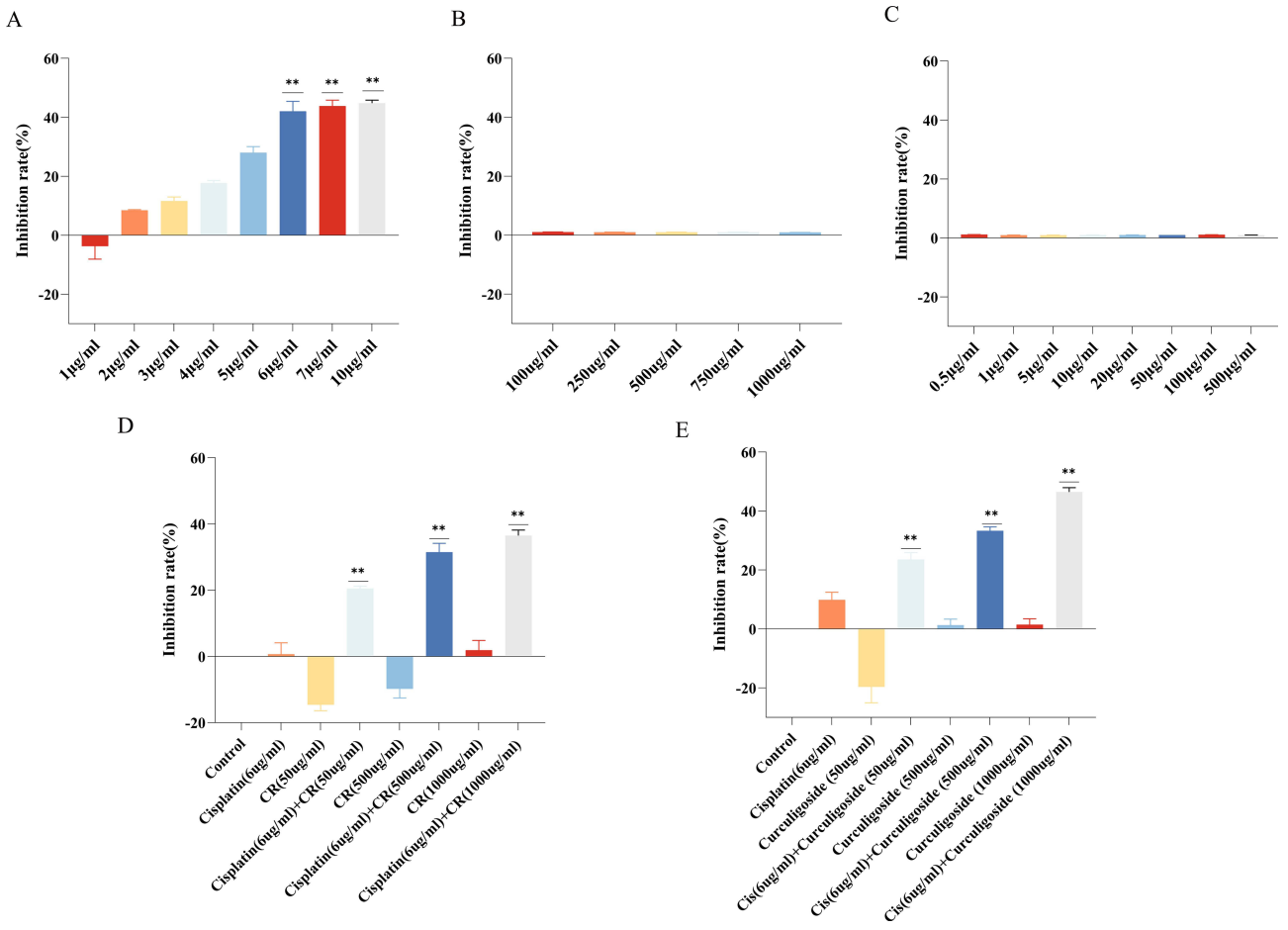

Figure 8 Cisplatin, CR,curculigoside alone and Cisplatin combined with CR/curculigoside inhibited A549/cis cell proliferation. (**A**) Effect of cisplatin alone on A549/cis cell viability; (**B**): Effect of Curculiginis Rhizoma alone on A549/cis cell viability; (**C**): Effect of curculigoside alone on A549/cis cell viability; (**D**): The effects of cisplatin, CR alone, and their combination on the proliferation rate of A549/cis cells; (**E**) The effects of cisplatin, curculigoside alone, and their combination on the proliferation rate of A549/cis cells. (**: P<0.01).

combined with both curculigoside and CR exhibited a reduction in cell viability and downregulated the expression of MRP, P-gp, and LRP in A549/cis cells. Notably, curculigoside demonstrated a remarkable downregulatory effect, particularly affecting the expression levels of MRP1, MRP2, MRP4, and LRP1. Besides, it has been proved in studies that Rhodamine 123 is the substrate of P-gp protein,[42] so we have detected the intracellular Rhodamine 123 content. The results showed that the use of cisplatin combined with CR/curculigoside can increase the accumulation of Rhodamine 123 in A549/cis cells.

However, the upstream core targets responsible for inducing the upregulation of MRP, LRP, and P-gp leading to resistance to platinum-based drugs remain unclear. The preliminary results of network pharmacology analysis revealed that among the highly significant gene targets in cisplatin treatment for lung cancer, JNK may have correlations with the regulation of MRP, LRP, and P-gp. JNK family, namely c-Jun N-terminal kinase, is one of the important protein families of MAPK. Activated JNK can bind to the transcription factor ATF2 and the N-terminal region of c-Jun, and phosphorylate the active region of transcription factor. In addition, these complexes bind to AP-1 (Activator protein 1) and AP-1-like sites on the promoters of many genes in the form of homodimer or heterodimer, increasing the transcriptional activity of AP-1 and promoting gene expression and protein synthesis.[43] Further literature studies revealed that JNK enhances the binding ability of its downstream target c-jun to the ABC binding cassette transporter and AP-1 site in the drug resistance protein promoter, promoting protein synthesis and multidrug resistance in tumor chemotherapy.[44–47] Bioinformatics analysis further demonstrated significant differences in JNK protein subtypes JNK1 and JNK2 in drug-

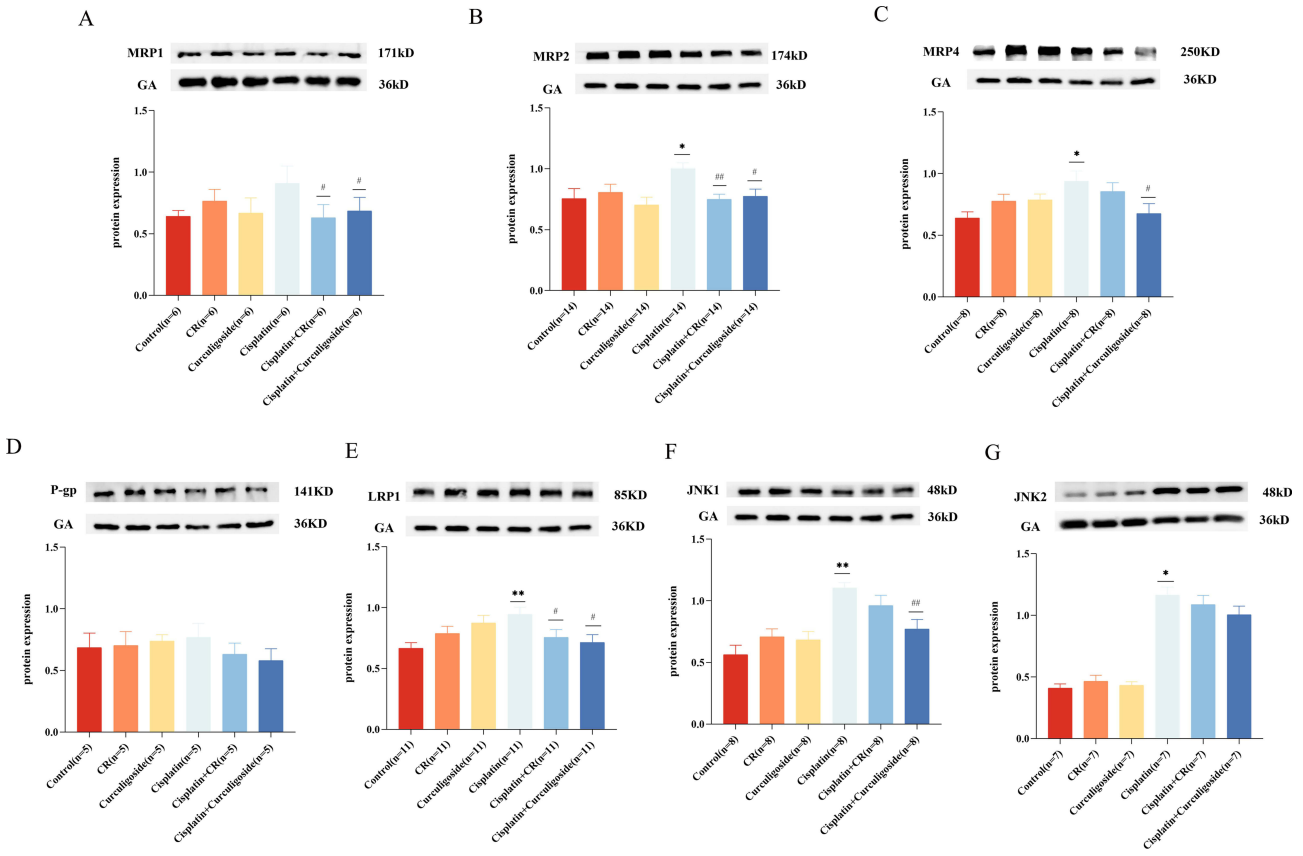

Figure 9 Inhibition of cisplatin-induced upregulation of JNK, MRP, LRP1, and P-gp by CR/curculigoside. (**A**) MRP1(n=6), (**B**) MRP2(n=14), (**C**) MRP4(n=8), (**D**) P-gp(n=5), (**E**) LRP1(n=11), (**F**) JNK1(n=8), (**G**) JNK2(n=7). (*: Comparison with the control group.P<0.05; **: Comparison with the control group.P<0.01; #: Compared with cisplatin group.P<0.05; ##: Compared with cisplatin group. P<0.01). Lanes of Figure 7B, 7E, and 7F came from the same blot, therefore the protein bands of GA are the same; Special Note: Due to glycosylation, the molecular weight of the MRP protein is greater than 250 kDa.

resistant and non-drug-resistant NSCLC cell lines. Additionally, high expression of JNK1 and JNK2 in NSCLC clinical samples correlated with worse overall survival rates, suggesting that these proteins may play pivotal roles in NSCLC drug resistance. On this basis, we performed cell experiments for verification. The results showed that the expressions of JNK1 and JNK2 were significantly decreased by Curculiginis Rhizoma water extract and curculigoside combined with cisplatin.

These findings indicate that curculigoside may function as the effective metabolite responsible for the suppression of cisplatin resistance in NSCLC by regulating the JNK-c-jun-MRP/LRP/P-gp signaling pathway, thereby impeding the development of multidrug resistance in cancer cells. However, it is important to note that the investigation did not explore the causal relationship between upstream and downstream proteins.

In conclusion, the utilization of an integrated research approach encompassing bioinformatics, molecular docking, molecular dynamics, in vivo and in vitro experiments has successfully elucidated the potential mechanism by which curculigoside counteracts cisplatin resistance in NSCLC. These findings establish a solid basis for conducting more comprehensive investigations into the anti-tumor resistance mechanism of curculigoside in future studies.

This experiment has only used methods such as bioinformatics, molecular docking, and molecular dynamics to preliminarily explore the mechanism of CR in improving cisplatin resistance in NSCLC at a theoretical level. Due to the complexity of drug–drug interactions and intracellular metabolic processes, subsequent studies still need to be conducted using techniques like mass spectrometry, in vitro and in vivo experiments, etc., to deeper investigate the mechanism of CR's sensitizing effect on cisplatin-resistant NSCLC, in order to enhance the rationality and scientificity of clinical medication.

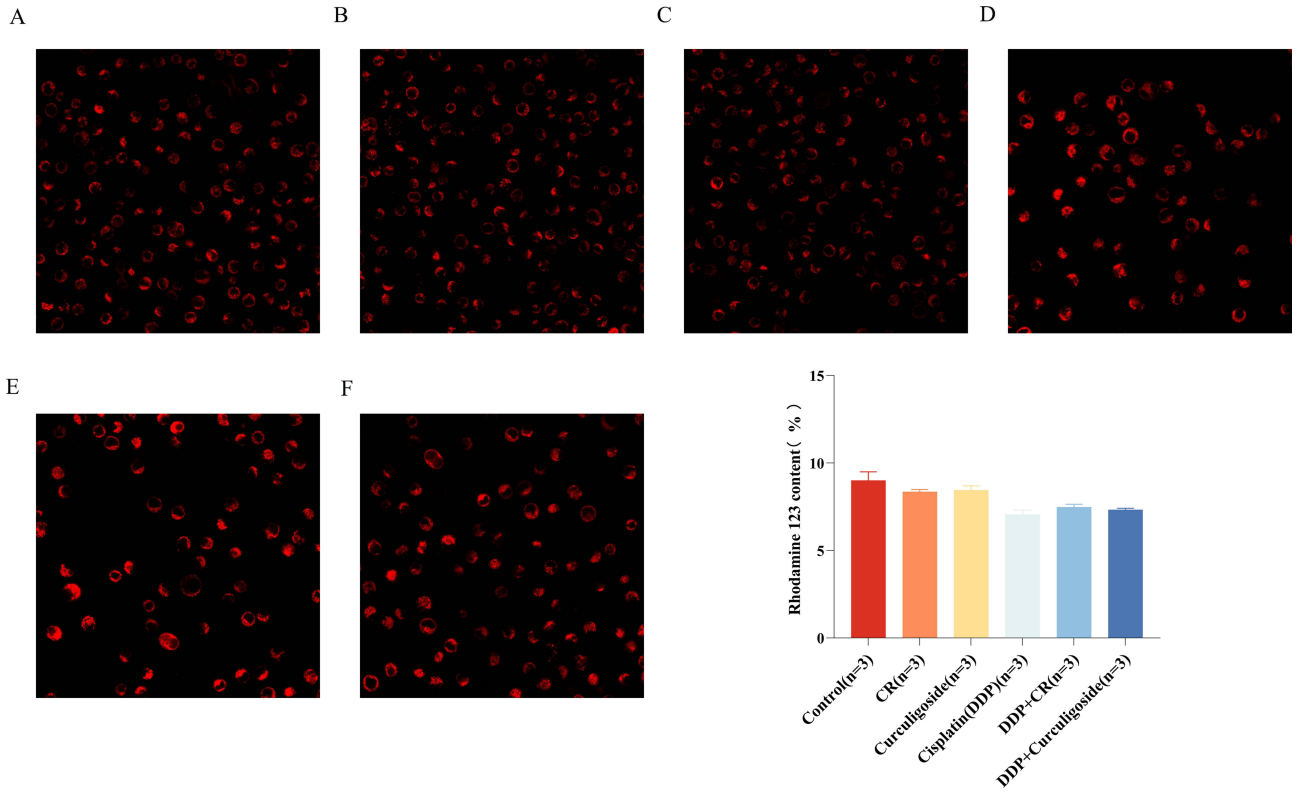

Figure 10 Rhodamine 123 is highly expressed in the cells by CR/curculigoside. (**A**) Control group(n=3), (**B**) CR group(n=3), (**C**) Curculigoside group(n=3), (**D**) Cisplatin group(n=3), (**E**) Cisplatin +CR group(n=3), (**F**) Cisplatin + curculigoside group(n=3).

Data Sharing Statement

The original contributions presented in the study are included in the article. Further inquiries can be directed to the corresponding author.

Funding

This study was supported by Dongzhimen Hospital, Beijing University of Traditional Chinese Medicine 2020 Annual Science and Technology Innovation Special Project (DZMKJCX-2020-004) and Beijing Pharmaceutical Association Clinical Pharmacy Research Project (LCYX-2022-01).

Disclosure

The authors declare that the research was conducted in the absence of any commercial or financial relationships that could be construed as a potential conflict of interest and approved by the Ethics Committee for exemption from ethical review.

References

1. Miller KD, Ortiz AP, Pinheiro PS, et al. Cancer statistics for the US Hispanic/Latino population, 2021. *CA Cancer J Clin*. 2021;71(6):466–487. doi:10.3322/caac.21695
2. Wu J, Lin Z. Non-Small Cell Lung Cancer Targeted Therapy: drugs and Mechanisms of Drug Resistance. *Int J Mol Sci*. 2022;23(23):15056. doi:10.3390/ijms232315056
3. Błach J, Wojas-Krawczyk K, Nicoś M, et al. Failure of immunotherapy-the molecular and immunological origin of immunotherapy resistance in lung cancer. *Int J Mol Sci*. 2021;22(16):9030. doi:10.3390/ijms22169030
4. Zhang CL, Zhu KP, Ma XL. Antisense lncRNA FOXC2-AS1 promotes doxorubicin resistance in osteosarcoma by increasing the expression of FOXC2. *Cancer Lett*. 2017;396:66–75. doi:10.1016/j.canlet.2017.03.018
5. Theodoulou FL, Kerr ID. ABC transporter research: going strong 40 years on. *Biochem Soc Trans*. 2015;43(5):1033–1040. doi:10.1042/BST20150139

6. Paolini A, Baldassarre A, Del Gaudio I, et al. Structural Features of the ATP-Binding Cassette (ABC) Transporter ABCA3. *Int J Mol Sci*. 2015;16(8):19631–19644. doi:10.3390/ijms160819631
7. Hellsberg E, Montanari F, Ecker GF. The ABC of Phytohormone Translocation. *Planta Med*. 2015;81(6):474–487. doi:10.1055/s-0035-1545880
8. Meschini S, Marra M, Calcabrini A, et al. Role of the lung resistance-related protein (LRP) in the drug sensitivity of cultured tumor cells. *Toxicol In Vitro*. 2002;16(4):389–398. doi:10.1016/s0887-2333(02)00035-8
9. Kryczka J, Kryczka J, Czarnecka-Chrebelska KH, et al. Molecular Mechanisms of Chemoresistance Induced by Cisplatin in NSCLC Cancer Therapy. *Int J Mol Sci*. 2021;22(16):8885. doi:10.3390/ijms22168885
10. Fan W, Shao K, Luo M. Structural View of Cryo-Electron Microscopy-Determined ATP-Binding Cassette Transporters in Human Multidrug Resistance. *Biomolecules*. 2024;14(2):231. doi:10.3390/biom14020231
11. Ou Z, Zhang Y, Wang Y. Research Progress on Pharmacological Mechanism of Curculigoside[J]. Guangdong Chemical Industry. 2023;50(05):117–119. Chinese
12. Chen J, Guo X, Liu X. Research progress on chemical constituents,pharmacological and toxicology effects of Curculigo orchioides Gaertn[J]. Journal of Traditional ChineseChinese Medicine. 2021;36(07):4151–4158. Chinese
13. Hao Y, Zhu B, Xue C. Sensitivity-enhancing Mechanism of Curculiginis Rhizoma in Cisplatin-resistant Non-small Cell Lung Cancer Cells Based on P-glycoprotein[J]. World Chinese Medicine. 2022;17(24):3462–3466+3471. Chinese
14. Weinstein JN, Collisson EA, Mills GB, et al.; Cancer Genome Atlas Research Network. The cancer genome atlas pan-cancer analysis project. *Nat Genet*. 2013;45(10):1113–1120. doi:10.1038/ng.2764
15. Fang L, Wang H, Li P. Systematic analysis reveals a lncRNA-mRNA co-expression network associated with platinum resistance in high-grade serous ovarian cancer. *Invest New Drugs*. 2018;36(2):187–194. doi:10.1007/s10637-017-0523-3
16. Byers LA, Diao L, Wang J, et al. An epithelial-mesenchymal transition gene signature predicts resistance to EGFR and PI3K inhibitors and identifies Axl as a therapeutic target for overcoming EGFR inhibitor resistance. *Clin Cancer Res*. 2013;19(1):279–290. doi:10.1158/1078-0432.CCR-12-1558
17. Dalvi MP, Wang L, Zhong R, et al. Taxane-platin-resistant lung cancers co-develop hypersensitivity to jumonjic demethylase inhibitors. *Cell Rep*. 2017;19(8):1669–1684. doi:10.1016/j.celrep.2017.04.077
18. Leek JT, Johnson WE, Parker HS, et al. The sva package for removing batch effects and other unwanted variation in high-throughput experiments. *Bioinformatics*. 2012;28(6):882–883. doi:10.1093/bioinformatics/bts034
19. Kassambara A, Kassambara MA. Package 'ggpubr'. *R Package Version 0.1*. 2020;6.
20. Kassambara A. Package 'survminer'. *Drawing Survival Curves Using 'ggplot2'(R Package Version*. 2017.
21. Dai YH, Wang YF, Shen PC, et al. Radiosensitivity index emerges as a potential biomarker for combined radiotherapy and immunotherapy. *NPJ Genom Med*. 2021;6(1):40. doi:10.1038/s41525-021-00200-0
22. Therneau TM, Lumley T. Package 'survival'. *R Top Doc*. 2015;128(10):28–33.
23. Fennell DA, Summers Y, Cadranel J, et al. Cisplatin in the modern era: the backbone of first-line chemotherapy for non-small cell lung cancer. *Cancer Treat Rev*. 2016;44:42–50. doi:10.1016/j.ctrv.2016.01.003
24. Galluzzi L, Senovilla L, Vitale I, et al. Molecular mechanisms of cisplatin resistance. *Oncogene*. 2012;31(15):1869–1883. doi:10.1038/onc.2011.384
25. Singh AP, Adrianzen Herrera D, Zhang Y, et al. Mouse models in squamous cell lung cancer: impact for drug discovery. *Expert Opin Drug Discov*. 2018;13(4):347–358. doi:10.1080/17460441.2018.1437137
26. Lim ZF, Ma PC. Emerging insights of tumor heterogeneity and drug resistance mechanisms in lung cancer targeted therapy. *J Hematol Oncol*. 2019;12(1):134. doi:10.1186/s13045-019-0818-2
27. Yi Q, Feng J, Liao Y, et al. Circular RNAs in chemotherapy resistance of lung cancer and their potential therapeutic application. *IUBMB Life*. 2023;75(3):225–237. doi:10.1002/iub.2624
28. Yan H, Tang S, Tang S, et al. miRNAs in anti-cancer drug resistance of non-small cell lung cancer: recent advances and future potential. *Front Pharmacol*. 2022;13:949566. doi:10.3389/fphar.2022.949566
29. Wang Y, Wang Y, Qin Z, et al. The role of non-coding RNAs in ABC transporters regulation and their clinical implications of multidrug resistance in cancer. *Expert Opin Drug Metab Toxicol*. 2021;17(3):291–306. doi:10.1080/17425255.2021.1887139
30. Dean M, Rzhetsky A, Allikmets R. The human ATP-binding cassette (ABC) transporter superfamily. *Genome Res*. 2001;11(7):1156–1166. doi:10.1101/gr.184901
31. Yang H, Yao J, Yin J, et al. Decreased LRIG1 in Human Ovarian Cancer Cell SKOV3 Upregulates MRP-1 and Contributes to the Chemoresistance of VP16. *Cancer Biother Radiopharm*. 2016;31(4):125–132. doi:10.1089/cbr.2015.1970
32. Liu X. *Study on the Expression and Clinical Meaning of LRP Genes in Non-Small Cell Lung Cancer*. Dalian Medical University; 2012. In Chinese.
33. Taheri M, Motalebzadeh J, Mahjoubi F. Expression of LRP Gene in Breast Cancer Patients Correlated with MRP1 as Two Independent Predictive Biomarkers in Breast Cancer. *Asian Pac J Cancer Prev*. 2018;19(11):3111–3115. doi:10.31557/APJCP.2018.19.11.3111
34. Zhang L, Li Y, Wang Q, et al. The PI3K subunits, P110α and P110β are potential targets for overcoming P-gp and BCRP-mediated MDR in cancer. *Mol Cancer*. 2020;19(1):10. doi:10.1186/s12943-019-1112-1
35. Lin H, Hu B, He X, et al. Overcoming Taxol-resistance in A549 cells: a comprehensive strategy of targeting P-gp transporter, AKT/ERK pathways, and cytochrome P450 enzyme CYP1B1 by 4-hydroxyemodin. *Biochem Pharmacol*. 2020;171:113733. doi:10.1016/j.bcp.2019
36. Adorni MP, Galetti M, La Monica S, et al. A New ABCB1 Inhibitor Enhances the Anticancer Effect of Doxorubicin in Both In Vitro and In Vivo Models of NSCLC. *Int J Mol Sci*. 2023;24(2):989. doi:10.3390/ijms24020989
37. Xiaoqing W, Chang L, Wenping L. Effects of Yiqi Huoxue Jiedu Fang on macrophage phenotype in patients with platinum-resistant ovarian cancer through regulating IL-6. *Journal of Beijing University of Traditional Chinese Medicine*. 2022;45(02):208–216. In Chinese.
38. Shen F, Jiayue X, Han F. Mechanism of Chinese Herbal Monomers Against Cisplatin-induced Resistance of Ovarian Cancer: A Review. *Chinese Journal of Experimental Traditional Medical Formulae*. 2022;28(03):226–233. In Chinese.
39. Zhang W, Mao X. Research progress on molecular compatibility in integrated Chinese and Western medicine to foster synergy and reverse resistance of cancer cells to anticancer drugs[J]. Chinese Journal of Clinical Oncology. 2021;48(11):566–570. Chinese
40. Zhu F, Zhang Y. Analysis of the effect of curculigoside on proliferation and differentiation of osteoblasts and the expression of inflammatory cytokines and its mechanism. *Chinese Journal of Osteoporosis*. 2019;25(5):642–648. In Chinese.

41. Cai K, Wang X. Effects of Curculigo orchioides polysaccharide on the immunity of immunocompromised mice induced by cyclophosphamide. *China J Trad Chin Med Pharm*. 2016;31(12):5030–5034. In Chinese.
42. Jouan E, Le Vée M, Mayati A, et al. Evaluation of P-Glycoprotein Inhibitory Potential Using a Rhodamine 123 Accumulation Assay. *Pharmaceutics*. 2016;8(2):12. doi:10.3390/pharmaceutics8020012
43. Sehgal V, Ram PT. Network Motifs in JNK Signaling. *Genes Cancer*. 2013;4(9–10):409–413. doi:10.1177/1947601913507577
44. Xu L, Fu Y, Li Y, et al. Cisplatin induces expression of drug resistance-related genes through c-jun N-terminal kinase pathway in human lung cancer cells. *Cancer Chemother Pharmacol*. 2017;80(2):235–242. doi:10.1007/s00280-017-3355-0
45. Tajitsu Y, Ikeda R, Nishizawa Y, et al. Molecular basis for the expression of major vault protein induced by hyperosmotic stress in SW620 human colon cancer cells. *Int J Mol Med*. 2013;32(3):703–708. doi:10.3892/ijmm.2013.1428
46. Skrypek N, Vasseur R, Vincent A, et al. The oncogenic receptor ErbB2 modulates gemcitabine and irinotecan/SN-38 chemoresistance of human pancreatic cancer cells via hCNT1 transporter and multidrug-resistance associated protein MRP-2. *Oncotarget*. 2015;6(13):10853–10867. doi:10.18632/oncotarget.3414
47. Zhang Y, Zhou J, Xu W, et al. JWA sensitizes P-glycoprotein-mediated drug-resistant choriocarcinoma cells to etoposide via JNK and mitochondrial-associated signal pathway. *J Toxic Environ Health A*. 2009;72(11–12):774–781. doi:10.1080/15287390902841649